Supporting Information for Qin et al., "Intermolecular Associations Determine the Dynamics of the Circadian KaiABC Oscillator"

SI Materials and Methods

Strains and *in vivo* rhythm measurement

Cyanobacterial strains were *Synechococcus elongatus* PCC7942 wild type and mutants that harbored different *kaiB* variants. Cells were grown and maintained as described previously (1). To create strains with *kaiB* variants, the *kaiB* ORF in the p*CkaiABC* plasmid (1) was mutagenized by site-directed PCR to replace the arginine residues at residues 22 and 74 with cysteine. The mutated p*CkaiABC* was then introduced into the *kaiABC*-deficient strain as described (1). Luminescence rhythm measurements as a reporter of circadian gene expression *in vivo* were as described previously (2).

Protein Preparation and Construction of KaiB and KaiC Variant Mutants

Kai proteins from *S. elongatus* were expressed in *Escherichia coli* and purified as described previously (3). The mutant variants of KaiB and KaiC proteins for expression in *E. coli* were constructed by site-directed mutagenesis (Stratagene, USA) of the vector plasmid pGEX-6P-1 (Amersham Biosciences, USA) harboring the appropriate *kai* gene. The KaiB mutant variants studied in this paper include $KaiB^{R22C}$ (arginine at residue 22 replaced with cysteine) and $KaiB^{R74C}$ (arginine at residue 74 replaced with cysteine). The KaiC mutant variants include $KaiC^{AA}$, $KaiC^{AE}$, $KaiC^{EE}$, $KaiC^{DA}$, $KaiC^{AT}$ and $KaiC^{DT}$, where the first superscript letter refers to the residue at site 431 (native KaiC has a serine at site 431) and the second letter refers to the residue at site 432 (native KaiC has a threonine at site 432). Therefore, native KaiC ($KaiC^{WT}$) would be labeled $KaiC^{ST}$ by this nomenclature. $KaiC^{489}$ was made by changing residue 490 to a stop codon so that the final 30 residues of the C-terminus were deleted; this mutation creates a KaiC that mimics hyperphosphorylated KaiC and can interact with KaiB alone, but cannot interact with KaiA alone because the C-terminal tentacles are missing (4).

Protein Concentration Measurement

The concentration of each protein was measured with the Bradford method (Bio-Rad Protein Assay) using a dilution series of bovine serum albumin (Bio-Rad) to generate a standard curve. The purity of each Kai protein was determined by analyzing the sample on SDS-PAGE gels.

In vitro KaiABC oscillation reactions and analysis of KaiC phosphoforms by SDS-PAGE

Reactions were carried out at 30ºC in reaction buffer (RB = 150 mM NaCl, 5 mM $MgCl_2$, 1 mM ATP, 0.5 mM EDTA, 50 mM Tris-HCl at pH 8.0) using the following Kai protein concentrations: 50-ng/μl KaiA, 50-ng/μl KaiB and 200-ng/μl KaiC. For analysis of KaiC phosphorylation status, samples (total 1μg KaiC at each time point) were collected from the *in vitro* reactions and resolved by SDS-PAGE (16 cm × 16 cm × 1mm gels with 10% acrylamide) at a constant current of 35 mA for 4-5 h. Gels were stained with colloidal Coomassie Brilliant Blue, and the gel images were digitally captured with the Gel Doc XR system (Bio-Rad). On each lane of the SDS-PAGE gels, the uppermost band is double phosphorylated KaiC (ST-KaiC), the next band down is KaiC that is phosphorylated on T432 (T-KaiC), the third band down is KaiC that is

phorphorylated on S431 (S-KaiC), and the bottommost band is non-phosphorylated KaiC (NP-KaiC). Quantity One (Bio-Rad) was used to quantify each phosphoform of KaiC from the gel images.

Analysis of Protein Interactions among Three Kai Proteins by Native-PAGE

Fig. 1 and Fig. 5 illustrate the method for analyzing the interaction between KaiB and KaiC (including mutant variants). KaiB (50 ng/μl) and KaiC (200 ng/μl) were incubated together at 30ºC in RB. For interaction among all three Kai proteins, KaiA (50 ng/μl) was also added. In the experiments of Figs. 2D and S3, complex formation between $KaiC^{489}$ and the three KaiB mutant variants was measured with the following concentrations: KaiB variant (500 ng/μl) and $KaiC^{489}$ (200 ng/μl). The 10X higher concentration of KaiB variants in this experiment was used to mimic the situation at the beginning of the phosphorylation phase, when KaiC phosphorylation is just beginning and KaiB would be in excess relative to the phosphorylated KaiC. $KaiC^{489}$ was used in the native-PAGE experiments to assay the KaiC-binding kinetics of the different KaiB variants because its mobility in native-PAGE is detectably different from that of KaiB (In native polyacrylamide gels, $KaiB^{WT}$ migrates to a similar position as the KaiB•KaiC complex, and consequently high concentrations of $KaiB^{WT}$ mask the signal of the KaiB•KaiC complexes in native-PAGE).

Aliquots (16μl) of the Kai protein mixtures were collected at each treatment/time point, combined with 5X native-PAGE sample buffer (50% glycerol, 0.05% bromophenol blue, 0.312M Tris-HCl at pH 6.8), flash-frozen in liquid nitrogen, and stored at -80 ºC. Native-PAGE (10 cm × 10 cm gels of 7.5% polyacrylamide gels) was performed in a cold room at 5mA constant current for 5 h to resolve protein complexes. Gels were stained with colloidal Coomassie Brilliant Blue, and gel images were digitally captured by Bio-Rad Gel Doc XR system. In Figs. 3A and S4, the protein density of the KaiC hexamer or the KaiA dimer was quantified by using Image J (NIH, USA). The initial KaiA density at time 0 was defined as 1, and the Complex Index at each time point was calculated by subtracting the density of KaiC from the initial density of KaiC. The Complex Index was then plotted as a function of time, and the free KaiA Index was plotted on the same graph (Fig. 3).

Fluorophore Labeling and Fluorescence Anisotropy

The fluorophore used to label the KaiA protein was fluorescein-5-maleimide (F-150, Invitrogen USA). A solution of F-150 was prepared in dimethyl sulfoxide, and the concentration was determined by using the extinction coefficient supplied by the manufacturer. Prior to labeling, KaiA protein in DTT-containing buffer (150mM NaCl, 1mM DTT, 50mM Tris-Cl, [pH 8.0]) was desalted on a G-25 Sephadex desalting column (GE Healthcare) equilibrated with the same buffer except without DTT. The desalted KaiA was labeled with F-150 at a 10:1 molar ratio for 2 h at room temperature in the dark and then overnight at 4 ºC. Unreacted fluorophore was removed from the fluorescently labeled KaiA protein with another G-25 Sephadex desalting column.

Fluorescence anisotropy (FA) was employed to determine the equilibrium dissociation constant (K_d) between the fluorescently labeled KaiA protein and the unlabeled KaiC protein. The labeled KaiA protein was 50-60 nM and the anisotropy was measured as a function of increasing concentrations of unlabeled KaiC protein after the two proteins were incubated for 30 min in the KaiABC reaction buffer (RB, see above) at 30ºC. Anisotropy measurements were made on a Photon Technology International spectrofluorimeter (T-format fluorometer).

Excitation and emission wavelengths were 490 and 515 nm, respectively. Anisotropy was measured using a time-based function for 10 s (integration time = 1 s), and the data were averaged. The binding between the KaiA dimer and KaiC hexamer proteins was assumed to be a 1:1 binding stoichiometry (5,6). The titration curves were fit to the following equation (7-9):

$$\Delta A = [(Y + S + K_d) - \{(Y + S + K_d)^2 - (4YS)\}^{1/2}] \cdot (A_{max} - A_{min})/(2Y)$$

Where ΔA = (the measured A) - (A_{min}), i.e., the change of the rotation of KaiA as a function of increasing [KaiC]. A is the measured anisotropy at a particular total concentration of the unlabeled KaiC protein (S) and the labeled KaiA protein (Y), A_{min} is the minimum anisotropy, A_{max} is the final maximum anisotropy, and K_d is the dissociation constant.

Electron microscopy of KaiA•KaiB•KaiC Complexes

The three KaiB variants were incubated with $KaiC^{EE}$ for 18 h at 30 degrees C. As described previously (3), samples were applied to glow discharged carbon coated EM grids and negatively stained with 0.75% uranyl formate. EM images were collected digitally on a 120KeV Tecnai12 LaB6 microscope at a 101,000x magnification using a Gatan 2kx2k US1000 camera. Individual particle images were selected and classified using ImagicV software and the EMAN software packages. The class sum images that appeared as complexes were generated from the following number of particle images for each of the KaiB variants: 2097 images for $KaiB^{WT}$, 1,517 images for $KaiB^{R22C}$, and 1,363 images for $KaiB^{R74C}$. These class sum average images are presented in Fig. 2E.

Mathematical Model Description

The mathematical model is similar to that described in the PTO model of Qin et al. 2010 (17). KaiC hexamer concentrations are labeled by net population phosphorylation levels, C_i, where i = 0, N. We neglect specific site-dependent modeling (S431 and T432) and treat the system phenomenologically. The model reactions are as follows:

Phosphorylation and de-phosphorylation:

Auto-phosphorylation/dephosphorylation :	$C_i \leftrightarrow C_{i+1}$
KaiA•KaiC phosphorylation//dephosphorylation:	$A•C_i \leftrightarrow A•C_{i+1}$
KaiB•KaiC, KaiA•KaiB•KaiC phosphorylation/dephosphorylation:	$B•C_{i+1} \leftrightarrow B•C_i$, $A•B•C_{i+1} \leftrightarrow A•B•C_i$

Hexamer Reactions:

KaiA association (and dissociation):	$A + C_i \leftrightarrow A•C_i$
	$A + B•C_i \leftrightarrow A•B•C_i$
KaiB association above threshold phosphorylation:	$B + C_i \leftrightarrow B•C_i \quad (i > N)$
Dissociation of KaiA•KaiB•KaiC complexes:	$B•A•C_0 \rightarrow B + A + C_0$
	$B•C_0 \rightarrow B + C_0$

Monomer Exchange (i + j = k+m):

$C_i + C_j \leftrightarrow C_k + C_m$

$A\bullet C_i + A\bullet C_j \leftrightarrow A\bullet C_k + A\bullet C_m$

$A\bullet B\bullet C_i + A\bullet B\bullet C_j \leftrightarrow A\bullet B\bullet C_k + A\bullet B\bullet C_m$

PTO Differential Equations: (i =1,N-1)

KaiC hexamers alone ($k_2 >> k_1$)

1.1 $dC_0/dt = -k_1 C_0 + k_2 C_1 - k_A A^*C_0 + k_{-A} (AC_0) + k_d (ABC_0) + k_d (BC_0)$

1.2 $dC_i/dt = k_1 (C_{i-1} - C_i) + k_2 (C_{i+1} - C_i) - k_A A^*C_i + k_{-A} (AC_i)$

1.3 $dC_N/dt = k_1 C_{N-1} - k_2 C_N - k_B B^*C_N + k_{-B} (BC_N) - k_A A^*C_N + k_{-A} (AC_N)$

KaiA-KaiC hexamers ($k_3 >> k_4$)

1.4 $d(AC_0)/dt = -k_3 (AC_0) + k_4 (AC_1) + k_A A^*C_0 - k_{-A} (AC_0)$

1.5 $d(AC_i)/dt = k_3 ((AC_{i-1}) - (AC_i)) + k_4 ((AC_{i+1}) - (AC_i)) + k_A A^*C_i - k_{-A} (AC_i)$

1.6 $d(AC_N)/dt = k_3 (AC_{N-1}) - k_4 (AC_N) + k_A A^*C_N - k_{-A} (AC_N)$

KaiB-KaiC ($k_2 >> k_1$)

1.7 $d(BC_N)/dt = k_B B^*C_N - k_{-B} (BC_N) - k_2 (BC_N) + k_1 (BC_{N-1}) - k_A A^*(BC_N)$

1.8 $d(BC_i)/dt = k_1 ((BC_{i-1}) - (BC_i)) + k_2 ((BC_{i+1}) - (BC_i)) - k_A A^*(BC_i)$

1.9 $d(BC_0)/dt = -k_1 (BC_0) + k_2 (BC_1) - k_d (BC_0) - k_A A^*(BC_0)$

KaiA-KaiB-KaiC ($k_2 >> k_1$)

1.10 $d(ABC_N)/dt = k_A A^*(BC_N) - k_2 (ABC_N) + k_1 (ABC_{N-1})$

1.11 $d(ABC_i)/dt = k_1 ((ABC_{i-1}) - (ABC_i)) + k_2 ((ABC_{i+1}) - (ABC_i)) + k_A A^*(BC_i)$

1.12 $d(ABC_0)/dt = -k_1 (ABC_0) + k_2 (ABC_1) - k_d (ABC_0) + k_A A^*(BC_0)$

KaiA ($k_A >> k_{-A}$)

1.13 $dA/dt = - k_A A^*(\Sigma C_i) - k_A A^*(\Sigma (BC_i)) + k_{-A} \Sigma (AC_i) + k_d (ABC_0)$

KaiB ($k_B >> k_{-B}$)

1.14 $dB/dt = -k_B B^*C_N + k_{-B} (BC_N) + k_d ((ABC_0) + (BC_0))$

Monomer Exchange

Monomer exchange is approximated phenomenologically by the reaction $C_i + C_j \rightarrow C_{i+1} + C_{j-1}$ (j >i) that acts to equalize the population concentration levels of phosphorylation by transfer of phosphates from hexamers with more phosphates (j) to hexamers with lower numbers of phosphates (i), j > i. Letting $x_k = C_k$, (AC_k), (BC_k), or (ABC_k):

1.15 $dx_i/dt = dx_i/dt - k_e x_i * x_j$ $(j = i+1, N)$

$dx_j/dt = dx_j/dt - k_e x_i * x_j$

$dx_{i+1}/dt = dx_{i+1}/dt + k_e x_i * x_j$

$dx_{j-1}/dt = dx_{j-1}/dt + k_e x_i * x_j$

PTO Initial Conditions and rates

All the differential equations are scaled to the initial KaiC concentration, C_0 (t=0) so that the fraction of each is followed with respect to time.

Simplified KaiA Sequesteration Model with Monomer exchange. The simplified model neglects the auto-phosphorylation/dephosphorylation reactions of KaiC (1.1 -1.3) and corresponding KaiB•KaiC complex formation reactions (1.7-1.9) and instead considers the approximate complex formation and cyclic phosphorylation reaction sequence:

1.16 $C_0 \rightarrow AC_0 \rightarrow AC_1 ... \rightarrow AC_N \rightarrow ABC_N \rightarrow ABC_{N-1} \rightarrow ... \rightarrow ABC_0 \rightarrow A+B+C_0$.

Monomer exchange occurs among A•C complexes (phosphorylation phase) and among A•B•C complexes (dephosphorylation phase) but not between the A•C complexes and the A•B•C complexes. The dynamics of this model are very similar to the full model in most simulations and provide a simpler interpretation of the resulting dynamics. However, the full model is required to adequately represent the time dependence of complex abundances reported previously (3,10). For the text figures we have used the simplified model.

Parameters for Figure 4

	phosphorylation (hr^{-1})	dephosphorylation(hr^{-1})
+ KaiA	$k_3 = 0.6$	$k_4 = 0.0$
+ KaiB	$k_1 = 0.0$	$k_2 = 0.6$

KaiA Association $k_A = 5.0$ (μM^{-1} hr^{-1})

KaiA Dissociation $k_{-A} = 0.0$ (hr^{-1})

KaiB Threshold $N = 6$

KaiB Association $k_B = 1.0$ (μM^{-1} hr^{-1})

KaiB Dissociation $k_{-B} = 1.0$ (hr^{-1})

KaiA-KaiB-KaiC Dissociation: $k_d = 1.0$ (hr^{-1})

	phosphorylation phase	dephosphorylation phase
Monomer Exchange (hr^{-1})	$k_{e1} = 2.5$	$k_{e2} = 5.0$

Figure 4C: As above except $k_{-B} = k_d = 1.0$; $k_{+B} = 0.25, 0.5, 1.0, 2.5, 5.0$ (different traces).

Simulations

Code for implementing the model was written in Fortran (G77, Free Software Foundation) using a 4th Order Runge-Kutta algorithm for ODE solutions.

Table S1

Properties of Wild-type and Mutant KaiA, KaiB, and KaiC Molecules

Version	Characteristics				Source or reference
	Period in vivo (hr)	Period in vitro	Protein interactions	ATPase activity (molecules per day)	
$KaiA^{WT}$	24.9 ± 0.10	Wild type	Binds KaiC and KaiBC complexes	Negligible (0.4) [13]	this study (ref.13)
$KaiB^{WT}$	24.9 ± 0.10	Wild type	Binds to KaiC	Negligible (0.4) [13]	this study (ref.13)
$KaiB^{R74C}$	21.7 ± 0.10	Shorten	Binds to KaiC	Data Not Available	this study
$KaiB^{R22C}$	26.2 ± 0.12	Lengthen	Binds to KaiC	Data Not Available	this study
$KaiC^{WT}$	24.9 ± 0.10	Wild type	Binds KaiB	12.6 ± 1.1 [13]; 14.5 ± 2.0 [14]	this study (refs.13,14)
$KaiC^{AA}$	Arhythmic [15]	Arhythmic [11]	Does not bind KaiB	27.1 ± 1.1 [13]; 26.8 ± 2.7 [14]	this study (refs.11, 13-15)
$KaiC^{AE}$	Not determined	Not determined	Does not bind KaiB	12.6 ± 1.1 [13]	this study (ref.13)
$KaiC^{DA}$	Not determined	Not determined	Does not bind KaiB	Data Not Available	this study
$KaiC^{EE}$ *	~ 40-50 [16]	Arhythmic	Binds KaiB	16.7 ± 0.8 [13]; 10.9 ± 0.3 [14]	this study (refs.13, 14, 16)
$KaiC^{AT}$	Arhythmic [15]	Arhythmic [11]	Does not bind KaiB	Data Not Available	this study (refs.11, 15)
$KaiC^{DT}$	Not determined	Arhythmic [11]	Binds KaiB	Data Not Available	this study (ref.11)
$KaiC^{489}$ **	Not determined	Not determined	Binds KaiB	59.6 ± 4.1 [13]	this study (ref.13)
* The data of ATPase activity is from $KaiC^{DE}$ ** The data of ATPase activity is from $KaiC^{487}$					

For the KaiC variants, the superscript letters refer to the residues at positions 431 and 432; "$KaiC^{WT}$" is wild-type or native KaiC in which residue 431 is serine and residue 432 is threonine. "$KaiC^{AE}$" is alanine at residue 431 and glutamate at residue 432, "$KaiC^{AT}$" is alanine at residue 431 and threonine at residue 432, "$KaiC^{EE}$" is glutamate at residues 431 and 432, and so on. "$KaiC^{489}$" is a truncated KaiC in which residue 490 was changed to a stop codon so that the final 30 amino acid residues were removed from the C-terminus of KaiC . For the KaiB variants, the superscript describes the entire mutation. For example, "$KaiB^{R74C}$" means that the arginine that normally resides at position 74 has been replaced with a cysteine.

Supplementary Figures

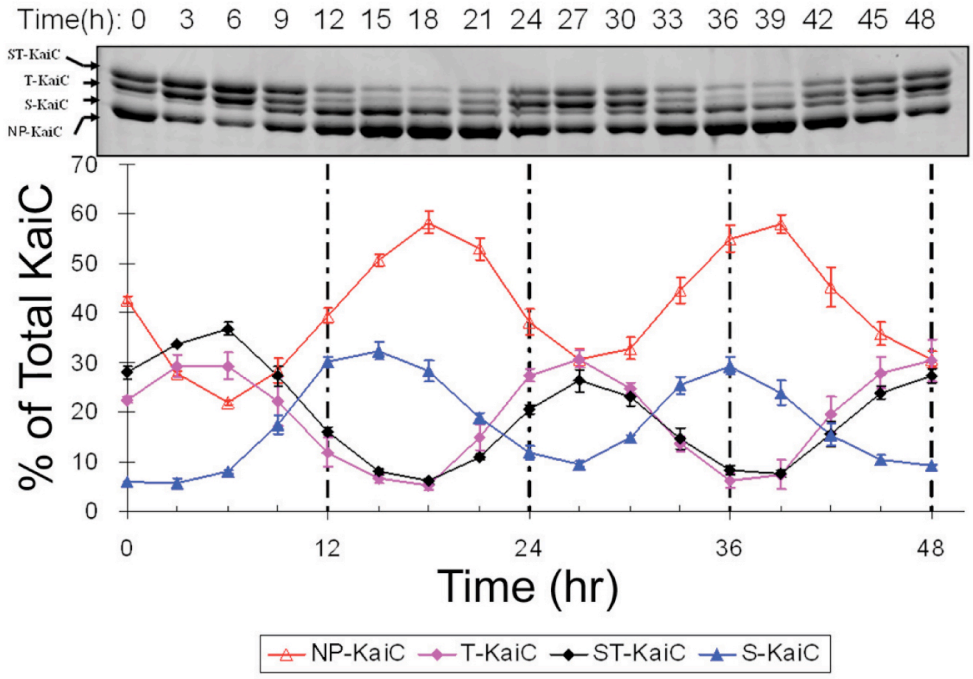

Fig. S1. Sequential phosphorylation events during the *in vitro* KaiABC oscillation. KaiC is sequentially phosphorylated during the *in vitro* cycle, first at T432 ("T-KaiC"), then at S431 ("ST-KaiC"), then T432 is de-phosphorylated ("S-KaiC"), followed by de-phosphorylation at S431 which returns KaiC to the hypophosphorylated state (nonphosphorylated KaiC, "NP-KaiC") (11,12). The upper panel is a SDS gel that depicts a representative KaiABC reaction for two days *in vitro*. The bottom panel is the densitometric analysis of each phosphoform of KaiC as a function of time from the beginning of the reaction (error bars are ± S.D. for three separate experiments). The sequential phosphorylation of KaiC is reproduced with the following order: NP-KaiC (Red), T-KaiC (Pink), ST-KaiC (Black), and S-KaiC (Blue).

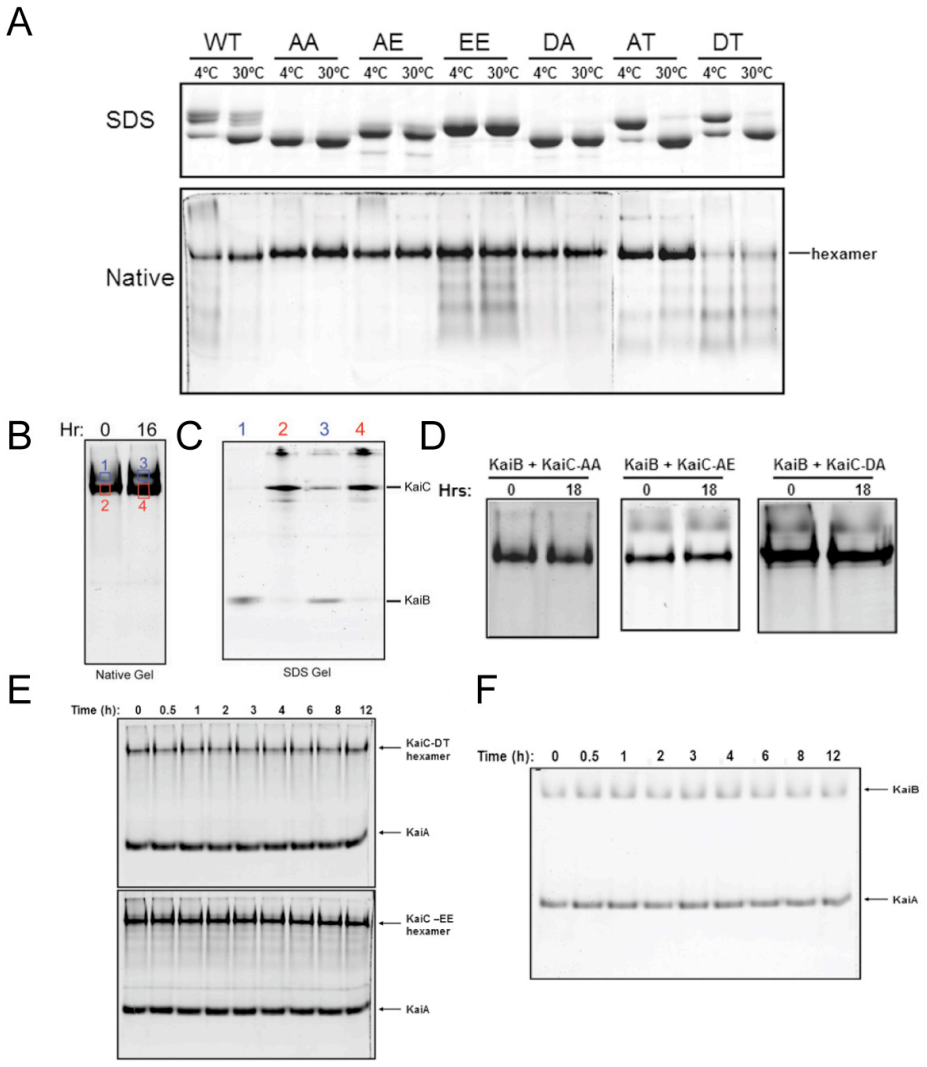

Fig. S2. Native gel electrophoresis of different combinations of Kai protein mutants. After proteins were mixed and incubated as described in the Methods for the indicated times, they were separated by electrophoresis in either SDS or native polyacrylamide gels. **(A)** Different phospho-mimics of KaiC were incubated at either 4°C or 30°C for 24 h, then separated by either SDS-PAGE (upper panel) or native-PAGE (lower panel). **(B,C)** KaiB forms complexes with $KaiC^{WT}$ protein. To identify the components of each band in the native gel (panel B), bands from the native gel were excised and resolved independently on a subsequent SDS-PAGE gel (panel C). Band #1 (blue box) is composed of only KaiB, bands #2 & 4 (red boxes) are composed of KaiC, and band#3 (blue box) is composed of both KaiB and KaiC (note that band#3 is shifted upwards from band#1). **(D)** KaiB does not form stable complexes with $KaiC^{AA}$, $KaiC^{AE}$, or $KaiC^{DA}$, as shown by the lack of a shifted band after an 18-h incubation. **(E)** KaiA does not form stable complexes with KaiC in the absence of KaiB. When KaiA is incubated with either KaiCDT or KaiCEE, there is no shift in the mobility of the KaiC hexamers and the density of the KaiA band is unchanged. **(F)** KaiB does not form a stable complex with KaiA in the absence of KaiC.

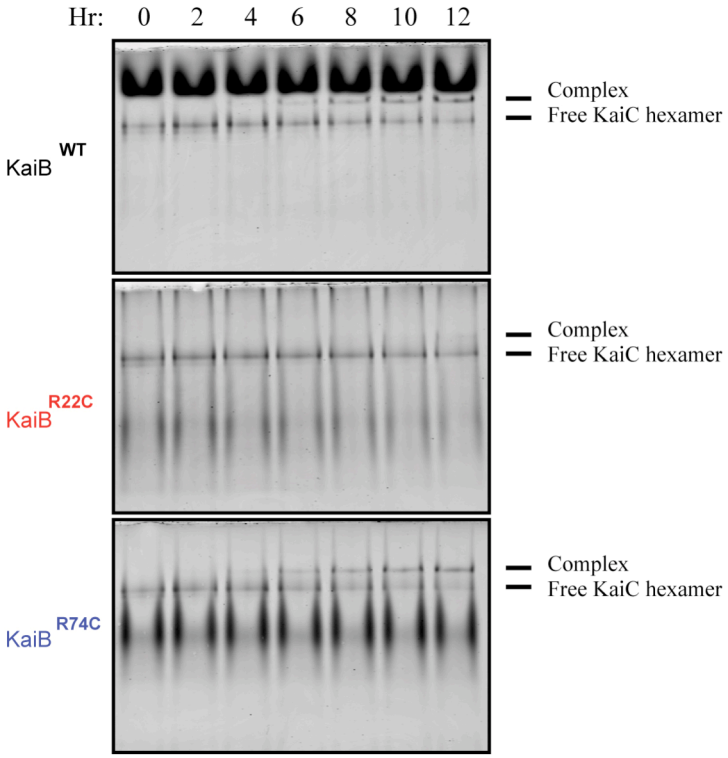

Fig. S3 (right). Formation of stable complexes between KaiC^{489} and the KaiB Variants. Native-PAGE analyses of time-dependent interactions between KaiC^{489} and KaiB^{R74C} (bottom panel), KaiB^{WT} (upper panel), and KaiB^{R22C} (middle panel). Incubations performed at 30ºC. These are the raw data of the plots in Fig. 2D.

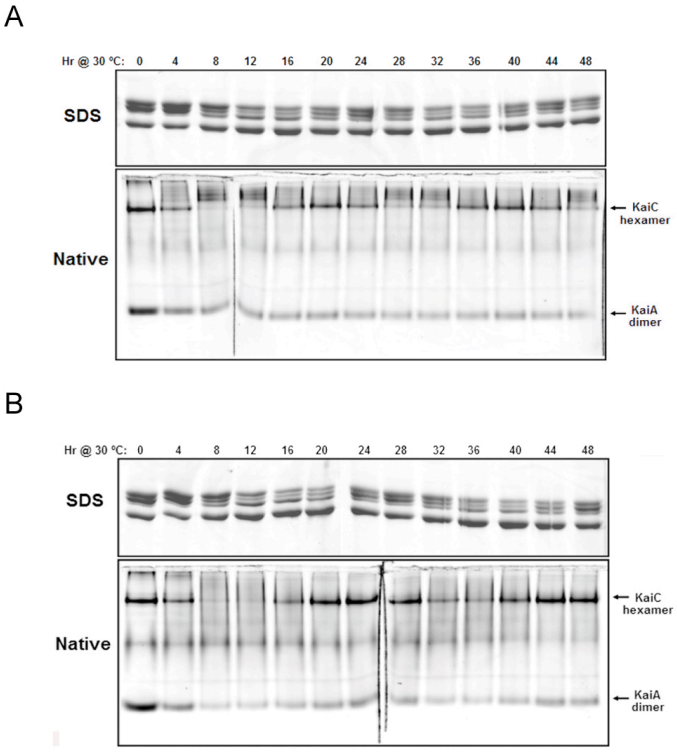

Fig. S4 (left). KaiA•KaiB•KaiC complexes rhythmically assemble and disassemble during the *in vitro* KaiABC oscillation with the KaiB^{R74C} and KaiB^{R22C} mutants. This supplementary figure is the raw data for Fig. 3 (panels B and D) and the procedure is the same as for Fig. 3A except for the use of the KaiB mutants as follows: **(A)** KaiB^{R74C} (short period), **(B)** KaiB^{R22C} (long period).

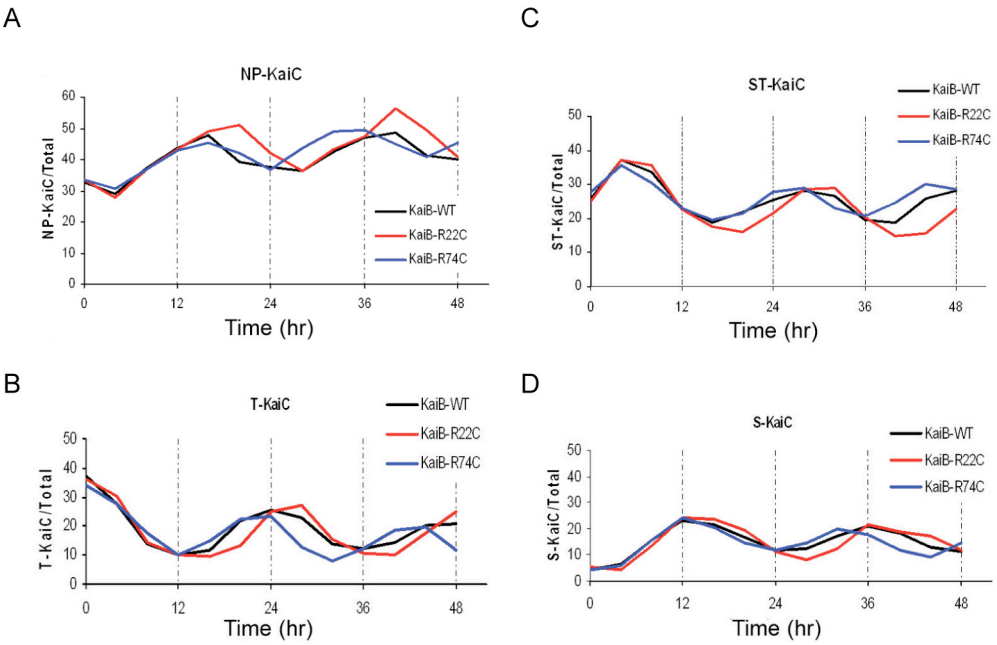

Fig. S5 (above). SDS-PAGE analyses of each KaiC phosphoform for all three KaiB mutant variants. Detailed analysis of each KaiC phosphoform as in Fig. S1 shows that the KaiB mutant variants change the period of the rhythms of : (**A**) hypophosphorylated KaiC (NP-KaiC), **(B)** KaiC phosphorylated on T432 (T-KaiC), **(C)** doubly-phosphorylated KaiC on both S431 and T432 (ST-KaiC), and **(D)** KaiC phosphorylated on S431 alone (S-KaiC).

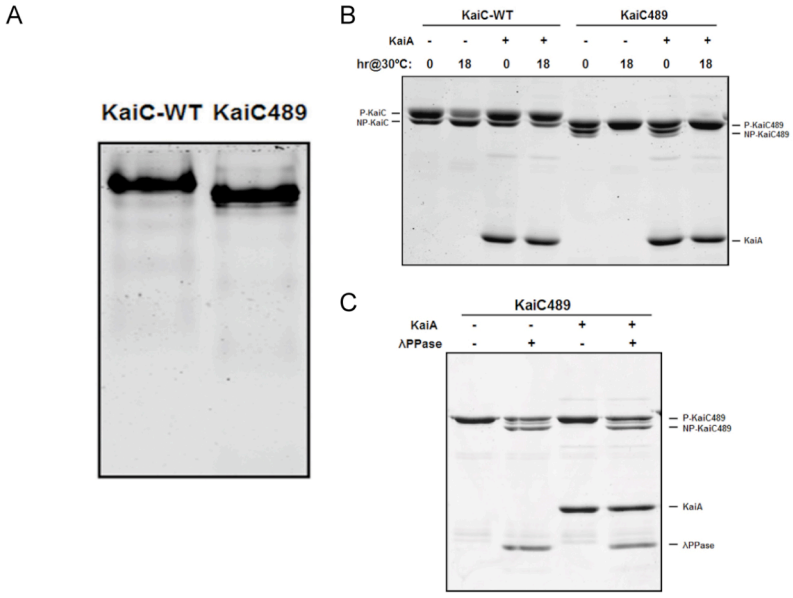

Fig. S6 (right). Characterization of hyperphosphorylated KaiC^{489}. **(A)** Native-PAGE indicates that KaiC^{489} forms hexamers as well as does KaiC^{WT}, and that its mobility is slightly higher than that of KaiC^{WT} due to the loss of the C-terminal tentacles. **(B)** KaiA enhances the auto-kinase activity of KaiC^{WT} at 30ºC. In the absence of KaiA, KaiC^{WT} becomes progressively less phosphorylated when incubated at 30ºC due to auto-phosphatase activity. However, KaiC^{489} does not auto-dephosphorylate in the absence of KaiA at 30ºC (in fact, it becomes progressively more phosphorylated), indicating that KaiC^{489} has low phosphatase activity (or at least that the auto-kinase activity can easily overbalance the auto-phosphatase activity). **(C)** Although the auto-phosphatase activity of KaiC^{489} is low, an external phosphatase (λPPase) is able to dephosphorylate KaiC^{489} in the absence or presence of KaiA.

References for Supporting Information

1. Ishiura M, et al. (1998) Expression of a gene cluster kaiABC as a circadian feedback process in cyanobacteria. *Science* 281: 1519-1523.
2. Xu Y, Mori T, Johnson CH (2003) Cyanobacterial circadian clockwork: roles of KaiA, KaiB and the kaiBC promoter in regulating KaiC. *EMBO J*. 22: 2117-26.
3. Mori T, et al. (2007) Elucidating the ticking of an in vitro circadian clockwork. *PLoS Biol* 5:e93.
4. Kim YI, Dong G, Carruthers CW Jr, Golden SS, LiWang A (2008) The day/night switch in KaiC, a central oscillator component of the circadian clock of cyanobacteria. *Proc Natl Acad Sci USA* 105: 12825-12830.
5. Pattanayek R, et al. (2006) Analysis of KaiA-KaiC protein interactions in the cyano-bacterial circadian clock using hybrid structural methods. *EMBO J* 25:2017-2028.
6. Hayashi F, et al. (2004) Stoichiometric interactions between cyanobacterial clock proteins KaiA and KaiC. *Biochem Biophys Res Commun* 316:195-202.
7. Müller B, Restle T, Reinstein J, Goody RS (1991) Interaction of fluorescently labeled dideoxynucleotides with HIV-1 reverse transcriptase. *Biochemistry* 30: 3709-3715.
8. Reid SL, Parry D, Liu HH, and Connolly BA (2001) Binding and recognition of GATATC target sequences by the EcoRV restriction endonuclease: a study using fluorescent oligonucleotides and fluorescence polarization. *Biochemistry* 40: 2484-2494.
9. Kovaleski BJ, et al. (2006) In vitro characterization of the interaction between HIV-1 Gag and human lysyl-tRNA synthetase. *J Biol Chem* 281: 19449-19456.
10. Kageyama H, et al. (2006) Cyanobacterial circadian pacemaker: Kai protein complex dynamics in the KaiC phosphorylation cycle in vitro. *Mol Cell* 23: 161-171.
11. Nishiwaki T, et al. (2007) A sequential program of dual phosphorylation of KaiC as a basis for circadian rhythm in cyanobacteria. *EMBO J* 26: 4029-4037.
12. Rust MJ, Markson JS, Lane WS, Fisher DS, O'Shea EK (2007) Ordered phosphorylation governs oscillation of a three-protein circadian clock. *Science* 318: 809-812.
13. Dong G, et al. (2010) Elevated ATPase activity of KaiC applies a circadian checkpoint on cell division in *Synechococcus elongatus*. *Cell* 140: 529-539.
14. Terauchi K, et al. (2007) ATPase activity of KaiC determines the basic timing for circadian clock of cyanobacteria. *Proc Natl Acad Sci USA* 104: 16377-16381.
15. Nishiwaki T, et al. (2004) Role of KaiC phosphorylation in the circadian clock system of *Synechococcus elongatus* PCC 7942. *Proc Natl Acad Sci USA* 101: 13927-13932.
16. Kitayama Y, Nishiwaki T, Terauchi K, Kondo T (2008) Dual KaiC-based oscillations constitute the circadian system of cyanobacteria. *Genes Dev* 22: 1513-1521.
17. Qin X, Byrne M, Xu Y, Mori T, Johnson CH (2010) Coupling of a Core Post-Translational Pacemaker to a Slave Transcription/Translation Feedback Loop in a Circadian System. *PLoS Biol* 8: e1000394.